

Title	Living microtransporter by uni-directional gliding of Mycoplasma along microtracks
Author(s)	Hiratsuka, Yuichi; Miyata, Makoto; Uyeda, Taro Q.P.
Citation	Biochemical and Biophysical Research Communications, 331(1): 318-324
Issue Date	2005-05-27
Type	Journal Article
Text version	author
URL	http://hdl.handle.net/10119/4965
Rights	NOTICE: This is the author's version of a work accepted for publication by Elsevier. Yuichi Hiratsuka, Makoto Miyata and Taro Q.P. Uyeda, Biochemical and Biophysical Research Communications, 331(1), 2005, 318-324, http://dx.doi.org/10.1016/j.bbrc.2005.03.168
Description	



Living microtransporter by uni-directional gliding of *Mycoplasma* along microtracks

Yuichi Hiratsuka¹, Makoto Miyata^{2,3}, Taro Q.P. Uyeda¹

¹Gene Function Research Center, National Institute of Advanced Industrial Science and Technology, 1-1-1 Higashi, Tsukuba, Ibaraki 305-8562, Japan,

²Department of Biology, Graduate School of Science, Osaka City University, and

³PRESTO, JST, Sumiyoshi-ku, Osaka 558-8585, Japan.

AUTHOR EMAIL ADDRESS: y-hiratsuka@aist.go.jp (YH),
miyata@sci.osaka-cu.ac.jp (MM), t-uyeda@aist.go.jp (TU)

CORRESPONDING AUTHOR FOOTNOTE: E-mail y-hiratsuka@aist.go.jp, phone +81-29-861-2555, fax +81-29-861-3048

Correspondence author:

Yuichi Hiratsuka

Gene Function Research Center.

National Institute of Advanced Industrial Science and Technology

Tsukuba Central 4

1-1-1 Higashi, Tsukuba, Ibaraki 305-8562, Japan

phone:+81-298-61-3048, fax: +81-298-61-3049

e-mail y-hiratsuka@aist.go.jp

ABSTRACT

The gliding bacterium *Mycoplasma mobile* adheres to plastic surfaces, and moves around vigorously. However, it has not been possible to control the direction of movements on plain surfaces. Here we report that, on patterned lithographic substrates, *M. mobile* cells are unable to climb tall walls, and move along the bottom edge of the walls. This property to move persistently along walls enabled us to design patterns that control direction of movements, resulting in uni-directional circling or one-way gating between two areas. Furthermore, cells loaded with streptavidin beads following biotinylation of surface proteins moved at normal speeds. These bacteria could be useful as living microtransporters, carrying cargo around within micrometer-scale spaces.

keywords: motor protein, bacterial motility, actuator, bottom up assembly, synthetic biology

INTRODUCTION

Miniaturization of devices to sizes that traditional mechanical engineering cannot handle demands innovative manufacturing processes and principles. Concerning miniature actuators and transporters, a number of synthetic approaches are currently pursued, including lithographically fabricated MEMS devices [1, 2], chemically synthesized molecular motors [3-5], and DNA mechanical devices [6, 7]. Turning our attention to biological world, diverse, efficient miniature actuators exist, such as flagellar motors of bacteria, F1ATPase involved in ATP synthesis, and eukaryotic motor proteins including myosin, kinesin, and dynein. Researches toward micro- or nano-actuators powered by those attractive biological molecules are actively proceeding now [8-12]. Especially, the kinesin-microtubule transport system, which can carry micrometer sized objects on solid surfaces in micrometer scaled areas, are expected as driving units for micro mechanical devices, such as delivery or material transport units in "lab-on-a-chip" devices. However, a number of

problems still remain. For example, efficient methods to assemble complex artificial devices using biological molecules do not yet exist. Moreover, such molecules are often unstable under artificial conditions. An alternative approach that we favor to circumvent those problems is the use of higher order biological motile systems, such as cells [13, 14] or organelles [15], rather than purified motor protein itself. We focused here on gliding bacteria, which are phylogenetically diverse and are abundant in many environments, move actively over solid surfaces using a process that does not involve flagella [16].

Mycoplasma mobile was isolated in 1981 from a lesion on the gill of the tench (*Tinca tinca*) as one species of gliding bacteria. The pear-shaped *M. mobile* cells are about 700 nm in length, 250 nm in diameter (at their widest) (**Fig. 1**). When *M. mobile* cells settle onto a host cell, or onto a glass or plastic surface in culture medium, they quickly adhere to the substrate surface and begin gliding while growing via binary fission. The tapered region is always at the front of gliding cells, and a

number of rod-like structures called “spikes” protrude from the tapered region and interact with the surface [17]. These spikes are believed to be the motile structures of this bacterium [18, 19]. The molecular mechanism of gliding remains unknown, though a mechanochemical walking model that makes use of the spikes has been proposed [18, 19]. As the name suggests, *M. mobile* cells have an outstanding ability to glide [20, 21], moving over surfaces at speeds up to 2~5 μm/s, which is more than five times faster than other species, and unlike those of other species the movements are continuous and uninterrupted by pauses.

Thus, *M. mobile* cells have a potential to serve as living microtransporters in artificial environments, with all the features of life such as capacities to self-organize, self-duplicate and self-repair when damaged. One of the problems that need to be solved towards this direction is the lack of methods to control the directions of their movements on surfaces. Here we report that *M. mobile* cells tend to move along the bottom of lithographic walls on surfaces, which allowed us to design patterns to

realize unidirectional circling or one way gating of these cells. We expect that this *M. mobile* motility system would be a potential alternative for the kinesin-microtubule motor system as microtransporters.

MATERIALS AND METHODS

Synthesis of the micropatterns— Polyurethane (NOA73, Norland, USA) micropatterned film was prepared on glass slides using the replica molding method [8, 22]. The master plates for the microstamps were made using electron-beam lithographically with an e-beam resist, SAL601 (Shipley Microelectronics, Japan), on silicon substrates. Polydimethylsiloxane (PDMS, Sylgard184, Dow Corning, USA) stamps were obtained by curing PDMS on the above master plate for 30 min at 120°C on a hotplate.

Construction of 50- to 1,200-nm-high step patterns— The master plates for a set of 50- to 1,200-nm-high step patterns were obtained by controlling the duration of etching with reactive ion etch (RIE) on silicon substrates.

Photolithographical patterns with about 20- μ m-thick resist, AZ5214-E (Clariant, Tokyo, Japan), were made on a silicon substrate, after which the unmasked surfaces were etched by RIE (Anelva, Japan, CF₄ gas 12.5 sccm, SF₆ gas 25 sccm, 5 Pa, 30 W) for 7 s (50 nm) to 160 s (1,200 nm). After removal of the residual resist with acetone, PDMS stamps were obtained

using the etched surfaces as templates. The steepness of the steps was checked by atomic force microscopy (data not shown).

Use of immunofluorescence to observe *M. mobile* movement— *M.*

mobile cells were cultured in Aluotto medium (2.1% heart infusion broth, 0.56% yeast extract and 10% serum) at 25°C [23]. To visualize the cells on microtracks, they were first immunochemically labeled with a mouse monoclonal antibody, mAb14, that recognized the surface proteins of the head and body regions of *M. mobile* [24], and then with a Cy3-conjugated anti-mouse secondary antibody (IgG) (Sigma-Aldrich). This immunofluorescent labelling procedure decreased the sliding velocity by approximately 20%, but we used this method for observation of movements along narrow linear channels because it was not possible to visualize individual cells clearly by the dark field optics on these line-patterned surfaces. To remove excess antibody, the mixture was centrifuged at 6,000 x g for 4 min, after which the pelleted cells were suspended in Aluotto medium by gentle trituration with a micropipette. The suspension

was then poured onto the patterned surface and left for 5 min to allow the cells to attach. The surface was then rinsed first with fresh medium to remove unbound cells and then with phosphate buffered saline (PBS; 74 mM sodium phosphate, 68 mM sodium chloride, pH 7.4) containing 20 mM glucose to minimize the background fluorescence.

Cargo attachment onto *M. mobile* cells— The culture medium of *M. mobile* was replaced with PBS containing 20 mM glucose. Surface proteins of *M. mobile* cells were functionalized by chemical modification using 25 μM biotin -polyethylene glycol-succinimide (Sharewater, USA) for 15 minutes at room temperature. After washing by pelleting and resuspending in fresh PBS twice, the biotinylated cells were frozen with liquid nitrogen and stored at -80 °C. Gliding activity of the cells was retained for at least two weeks under this storage condition. Streptavidin coated polystyrene beads were prepared by according to the protocol of Calbodiimide Kit for carboxylated microparticles (Polyscience, Inc., USA). To attach beads onto *M. mobile* cells, equal volumes of suspension of *M.*

mobile cells (1×10^6 cells/l) and that of the streptavidin-immobilized beads (2×10^6 particles/l) in PBS containing 20 mM glucose were mixed, and after 15 min of incubation, a third volume of the culture medium containing 1 mM biotin was added to stop the reaction. This condition allowed more than 90% of the cells to bind to one or more beads, and the rate constant of this reaction corresponds to the diffusion-limited reaction rate constant ($\sim 10^9 \text{ M}^{-1} \text{ s}^{-1}$) calculated from the Smoluchowski-Debye equation. This indicates that most of the collision events between an *M. mobile* cell and a bead in the reaction mixture led to formation of tight cell/bead complex via the biotin-streptavidin interaction. This high efficiency should be, at least in part, due to the long linker of polyethylene glycol (stretched length ~ 20 nm) between the biotin and succinimide portions, because a long linker with a high degree of freedom in motion was very effective to accelerate binding reactions between poorly diffusive solid and solid micro-objects, such as micro particles and macromolecular protein assemblies [25].

RESULTS AND DISCUSSIONS

When we cultured *M. mobile* cells on micropatterned surfaces having vertical steps prepared by replica molding [22], we found that the directions of the cells' movements were profoundly affected by the pattern geometry (**Fig. 2a**). When an *M. mobile* cell moving over the flat bottom bumped against a step, it either climbed the step or changed direction and continued to glide on the bottom along the wall created by the step. The probability of the non-climbing change in direction was related to the approach angle and the height of the step (**Fig. 2b**). In general, higher steps and shallower approach angles favored non-climbing changes in direction. Moreover, *M. mobile* cells could not climb steps higher than 1,200 nm, irrespective of the approach angle, indicating that the motion of all *M. mobile* cells can be efficiently confined within an area surrounded by walls higher than 1,200 nm. It is noteworthy that when they did not climb the step, *M. mobile* cells typically glided along bottom edge of the wall, rather than out to the open area away from the wall. We speculate that a

larger number of spikes can attach to the intersecting surfaces at the bottom edge of a wall than to a single flat surface, and that this stabilizes the cells' movements along the bottoms of walls. To evaluate the persistency of *M. mobile* cells to move along curved walls, we observed movements of the cells along two linear walls interrupted by an outward 180-degree turn away from the cells. Majority of the cells moved around the corner when the curvature radius was larger than 2 μ m. In contrast, majority of the cells dissociated from the pattern and moved straightly when the radius was 50 nm (**Table 1**).

Within narrow, linear channels (500 nm wide and 800 nm deep), most *M. mobile* cells glided continuously, without changing direction (**Fig. 2c** and **Supplementary Video 2** online), at an average velocity of $2.30 \pm 0.57 \mu$ m/s (N=171), which was equal to the velocity on flat surfaces ($2.28 \pm 0.36 \mu$ m/s; N=91). When two cells moving in opposite directions met within a channel, one of two things happened. In the majority of cases they passed by one another as if nothing had occurred (**Fig. 2c**, arrowhead).

This is reasonable because the channels are roughly twice as wide as typical *M. mobile* cells. In some cases, however, one of the cells gave way and moved to the adjacent lane, probably due to collision (**Fig. 2d**, red cell indicated by arrow). Collisions were also observed between cells gliding in the same direction at different speeds. In the case shown in Figure 2e (arrowhead), the faster cell (yellow) moved to the adjacent lane after bumping into the rear of the slower cell (green).

We next designed a pattern for unidirectional movement of *M. mobile*, which consisted of repetitive broken circles connected by lines (**Fig. 3a**). With this configuration, an *M. mobile* cell moving around in the larger open spaces eventually reached one of the elevated line patterns and began to move along it. Both ends of the line were curved to introduce the cell into the circular pattern (**Fig. 3b**). The ends of the lines were made sharp with a curvature radius of approximately 50 nm (**Fig. 3d**), so that 70~99% of the cells dissociated from the line and moved straight to the next line in a counter-clockwise direction. This geometry caused most

cells to keep moving in a counter-clockwise direction along the inner walls of the broken circular line patterns. By contrast, a cell moving in the incorrect (clockwise) direction within a broken circle would escape by moving along the straight line, but would enter the neighboring broken circle in the correct direction. As a result, 90.6 ± 8.1 % (average from eight independent patterns) of *M. mobile* cells on the surface rotated unidirectionally in a counter-clockwise direction along the broken circle patterns (**Fig. 3c** and **Supplementary Video 3** online).

Other simple asymmetric patterns also affected the direction of *M. mobile* movements in interesting ways. For example, aligned crescent or tear drop patterns functioned as one-way gates, or Maxwell's demon, because cells moving on either side would eventually reach the patterns, glide along the wall and dissociate from the pattern only on the side with sharp ends (**Fig. 3e, f**). Thus, randomly moving *M. mobile* cells within two square regions separated by aligned crescent patterns gradually accumulated in the left compartment (**Fig. 3g, h**). With this pattern, 75.9

$\pm 9.2\%$ (N=5) of the cells were concentrated in the left square after 20 min.

Finally, we demonstrated the ability of *M. mobile* cells to transport artificial micrometer-sized objects. It has been already reported that *M. mobile* cells can be loaded with a micrometer sized-bead via specific antibodies and carry it around at normal speeds [26], but this binding reaction was rather inefficient. We thus developed an efficient method to harness the biotin-avidin linkage system to *M. mobile* cells and to form one to one complexes of cells and streptavidin-conjugated beads. Surface of *M. mobile* cells was biotinylated using biotin-polyethylene glycol-succinimide ester that specifically reacts with lysine residues of protein. The covalently biotinylated cells were then mixed with 0.5 μ m micro bead conjugated with streptavidin. With the optimized cell to bead ratio and reaction time, 62% of the cells had one bound bead (**Fig. 4b-d**), while 9% had none (**Fig. 4a**), and the remainder were in multiplex complexes (**Fig. 4e**).

The gliding velocities of cells carrying one or two beads were 3.26

± 1.37 and 3.40 ± 0.94 μ m/sec, respectively, which were not slower than unloaded cells (3.37 ± 1.02 μ m/s) (n=50 for each type of cells) (**Fig. 4f-k** and **Supplementary Video 4** online). This is reasonable, since 27 pN stall force generated by an *M. mobile* cell [26] is a thousand fold greater than a viscous drag force on a bead with 0.5 μ m diameter moving at 3 μ m/s in water. In theory, one *M. mobile* cell should be able to carry an object with the size of tens of micrometers without a significant loss of the gliding speed.

Research aimed at realization of nano- and microactuators powered by motor proteins is actively progressing [8-12, 27-30]. In particular, directional transport by kinesin-microtubule motors over surfaces is thought to be a possible basis for conveyor-belt-like transporters in miniature bioreactors or lab-on-a-chip type devices [8, 9, 12]. We point out that the motile properties of *M. mobile* cells are comparable with, or perhaps superior to, the current kinesin/microtubule systems (**Table 2**), and the methods to control direction of *M. mobile* movements are now

presented. Based on these comparisons, we propose that the gliding motility of *M. mobile* also has the potential to serve as the basis for microtransporters of this type.

While there are many potential advantages to using defined materials derived from living organisms to build integrated nano- or micro devices, one serious disadvantage, especially of proteins, is their fragility once they are isolated from living cells. The motility of *M. mobile* is robust and superior to that of the purified motor proteins in that regard. This is because in the *M. mobile* system, the cell, itself, functions as the actuator with all the features of a living organism (e.g., reproduction and self-repair). Furthermore, use of *M. mobile* cells or other higher order biological structures as motile devices or actuators alleviates many of the problems associated with the assembly of complex devices and systems from multiple biological molecules and synthetic nanocomponents. Finally, since genetic manipulation or modification of *M. mobile* functions will likely be necessary to realize mechanical devices powered by the cells,

it is helpful that the mycoplasma genome is one of the simplest [31]. We expect that *M. mobile*, “domesticated” by molecular genetic methods, will eventually serve as the basis for microtransporters or microlocomotives that are able to reproduce and to repair themselves.

ACKNOWLEDGMENTS

We thank Dr. T. Tada for advice on microfabrication processes, Dr. N. Kanzaki for taking the atomic force micrographs of the patterns, and Dr. A. Uenoyama for helpful discussions about the properties of *M. mobile*.

This work was supported in part by Grants-in-Aid for Scientific Research and for Science Research on Priority Area from the Ministry of Education, Culture, Sports, Science and Technology to M.M.

REFERENCES

- [1] J. M. Bustillo, R. T. Howe, and R. S. Muller, Surface micromachining for microelectromechanical systems, *Proc. IEEE* 86 (1998) 1552-1574.
- [2] M. Mehregany, S. F. Bart, L. S. Tavrow, J. H. Lang, S. D. Senturia, and M. F. Schlecht, A Study of Three Microfabricated Variable-Capacitance Motors, Sensors and Actuators a 21 (1990) 173-179.
- [3] M. C. Jimenez, C. Dietrich-Buchecker, and J. P. Sauvage, Towards Synthetic Molecular Muscles, *Angew. Chem. Int. Ed.* 39 (2000) 3284-3287.
- [4] N. Koumura, R. W. Zijlstra, R. A. van Delden, N. Harada, and B. L. Feringa, Light-driven monodirectional molecular rotor, *Nature* 401 (1999) 152-155.
- [5] D. A. Leigh, J. K. Wong, F. Dehez, and F. Zerbetto, Unidirectional rotation in a mechanically interlocked molecular rotor, *Nature* 424 (2003) 174-179.
- [6] B. Yurke, A. J. Turberfield, A. P. Mills, Jr., F. C. Simmel, and J. L.

Neumann, A DNA-fuelled molecular machine made of DNA, *Nature* 406 (2000) 605-608.

[7] H. Yan, X. Zhang, Z. Shen, and N. C. Seeman, A robust DNA mechanical device controlled by hybridization topology, *Nature* 415 (2002) 62-65.

[8] H. Hess, J. Clemmens, D. Qin, J. Howard, and V. Vogel, Light-controlled molecular shuttles made from motor proteins carrying cargo on engineered surfaces, *Nano Letters* 1 (2001) 235-239.

[9] Y. Hiratsuka, T. Tada, K. Oiwa, T. Kanayama, and T. Q. P. Uyeda, Controlling the direction of kinesin-driven microtubule movements along microlithographic tracks, *Biophys. J.* 81 (2001) 1555-1561.

[10] L. Limberis, J. J. Magda, and R. J. Stewart, Polarized alignment and surface immobilization of microtubules for kinesin-powered nanodevices, *Nano Letters* 1 (2001) 277-280.

[11] K. J. Bohm, R. Stracke, P. Muhlig, and E. Unger, Motor protein-driven unidirectional transport of micrometer-sized cargoes across

isopolar microtubule arrays, *Nanotechnology* 12 (2001) 238-244.

[12] L. L. Jia, S. G. Moorjani, T. N. Jackson, and W. O. Hancock, Microscale transport and sorting by kinesin molecular motors, *Biomed. Microdevices* 6 (2004) 67-74.

[13] N. Darnton, L. Turner, K. Breuer, and H. C. Berg, Moving fluid with bacterial carpets, *Biophys J* 86 (2004) 1863-1870.

[14] J. Xi, J. J. Schmidt, and C. D. Montemagno, Self-assembled microdevices driven by muscle, *Nat Mater* 4 (2005) 180-184.

[15] M. Knoblauch, G. A. Noll, T. Muller, D. Prufer, I. Schneider-Huther, D. Scharner, A. J. Van Bel, and W. S. Peters, ATP-independent contractile proteins from plants, *Nat Mater* 2 (2003) 600-603.

[16] M. J. McBride, Bacterial gliding motility: multiple mechanisms for cell movement over surfaces, *Annu. Rev. Microbiol.* 55 (2001) 49-75.

[17] M. Miyata, and J. D. Petersen, Spike Structure at the Interface between Gliding *Mycoplasma mobile* Cells and Glass Surfaces Visualized by Rapid-Freeze-and-Fracture Electron Microscopy, *Journal of Bacteriology*

186 (2004) 4382-4386.

[18] A. Uenoyama, A. Kusumoto, and M. Miyata, Identification of a 349-kilodalton protein (Gli349) responsible for cytoadherence and glass binding during gliding of *Mycoplasma mobile*, *J. Bacteriol.* 186 (2004) 1537-1545.

[19] M. Miyata, Gliding motility of mycoplasmas - A mechanism cannot be explained by today's biology -. in *Mycoplasmas: pathogenesis, molecular biology, and emerging strategies for control*, in Blanchard, A., and Browning, G., (Eds.), Horizon Scientific Press, Norwich, 2005, pp. 12345-67890.

[20] H. Kirchhoff, P. Beyene, M. Fischer, J. Flossdorf, J. Heitmann, B. Khattab, D. Lopatta, R. Rosengarten, G. Seidel, and C. Yousef, *Mycoplasma mobile* sp. nov., a new species from fish, *Int. J. Syst. Bacteriol.* 37 (1987) 192-197.

[21] H. Kirchhoff, U. Boldt, R. Rosengarten, and A. Kleinstruckmeier, Chemotactic response of a gliding mycoplasma, *Curr. Microbiol.* 15 (1987)

57-60.

[22] Y. N. Xia, and G. M. Whitesides, Soft lithography, *Angew. Chem. Int. Ed.* 37 (1998) 551-575.

[23] B. B. Aluotto, R. G. Wittler, C. O. Williams, and J. E. Faber, Standardized bacteriologic techniques for the characterization of mycoplasma species., *Int. J. Syst. Bacteriol.* 20 (1970) 35-58.

[24] A. Kusumoto, S. Seto, J. D. Jaffe, and M. Miyata, Cell surface differentiation of *Mycoplasma mobile* visualized by surface protein., *Microbiology* (2004) *in press*.

[25] Y. Z. Du, Y. Hiratsuka, T. Q. P. Uyeda, N. Yumoto, and M. Kodaka, Motor protein nano-biomachine powered by self-supplying ATP, *Chem. Commun.* (2004) *in press*.

[26] M. Miyata, W. S. Ryu, and H. C. Berg, Force and velocity of *Mycoplasma mobile* gliding, *J. Bacteriol.* 184 (2002) 1827-1831.

[27] R. Bunk, J. Klinth, L. Montelius, I. A. Nicholls, P. Omling, S. Tagerud, and A. Mansson, Actomyosin motility on nanostructured surfaces,

Biochem. Biophys. Res. Commun. 301 (2003) 783-788.

[28] H. Suzuki, A. Yamada, K. Oiwa, H. Nakayama, and S. Mashiko,

Control of actin moving trajectory by patterned poly(methyl methacrylate) tracks, Biophys. J. 72 (1997) 1997-2001.

[29] R. K. Soong, G. D. Bachand, H. P. Neves, A. G. Olkhovets, H. G.

Craighead, and C. D. Montemagno, Powering an inorganic nanodevice with a biomolecular motor, Science 290 (2000) 1555-1558.

[30] H. Liu, S. J.J., G. D. Bachand, S. S. Rizk, L. L. Looge, H. W. Hellinga,

and C. D. Montemagno, Control of a biomolecular motorpowered nanodevice with an engineered chemical switch, Nat. Mater. 1 (2002) 173-177.

[31] S. Razin, D. Yogeve, and Y. Naot, Molecular biology and pathogenicity of mycoplasmas, Microbiol. Mol. Biol. Rev. 62 (1998) 1094-1156.

[32] K. Visscher, M. J. Schnitzer, and S. M. Block, Single kinesin

molecules studied with a molecular force clamp, Nature 400 (1999) 184-189.

[33] V. S. Reddy, and A. S. Reddy, The calmodulin-binding domain from a plant kinesin functions as a modular domain in conferring Ca²⁺-calmodulin regulation to animal plus- and minus-end kinesins, *J. Biol. Chem.* 277 (2002) 48058-48065.

[34] C. Brunner, K. H. Ernst, H. Hess, and V. Vogel, Lifetime of biomolecules in polymer-based hybrid nanodevices, *Nanotechnology* 15 (2004) S540-S548.

FIGURE LEGENDS

Figure 1

Morphology of *Mycoplasma mobile*. Rapid-freeze-and-fracture rotary-shadow electron micrograph of a *Mycoplasma mobile* cell (scale bar, 100 nm), modified from reference [17]. *M. mobile* cells glide in the direction indicated by the arrow. Rod-like “spikes” comprised of motor proteins protrude from the tapered region (arrowheads). A video for the movements of *M. mobile* cells over a flat surface is available on web site **(supplementary Video 1)**.

Figure 2

Behaviors of the cells' movements around vertical steps. **(a)** Scheme of the movement of *M. mobile* on a surface with a vertical step. When a *M. mobile* cell arrives at the base of the step, it either climbs up the wall or glides along it. **(b)** The probabilities of non-climbing when motile *M. mobile* cells hit the bottom of steps were scored as a function of the

approach angle (between ± 7.5 degrees of the indicated angle) and the height of the step (open circles, 50 nm; open triangles, 100 nm; open squares, 200 nm; closed triangles, 400 nm; closed squares, 800 nm; and closed circles, 1,200 nm). (c-e) Movement of *M. mobile* cells along narrow linear channels. Time-lapse fluorescence micrographs showing the movement of *M. mobile* cells within 500-nm-wide, 800-nm-deep linear channels (scale bar, 4 μ m). Selected cells are colored to help tracking. Two cells moving in opposite directions in the same channel lane either bypassed one another (panel c, green and cyan and then green and red; both are indicated by arrowheads) or collided, which caused one of the cells to change lanes (panel d, red and green; arrow). When a faster cell collided with a slower one from behind, it moved to the next lane but kept moving in the same direction (panel d, green and yellow; arrowhead). Atomic force micrograph of the linear channels (e). See a supplementary video 2.

Figure 3

Use of asymmetric patterns to elicit unidirectional movement along circular tracks and one-way gating with *M. mobile* cells. **(a)** Scanning electron micrograph of the repetitive broken circular pattern for unidirectional rotational movement. Scale bar, 10 μ m. **(b)** A schematic image of the mechanism by which unidirectional rotation within the repetitive circular pattern is achieved. An *M. mobile* cell moving along the linear track enters the pattern in the correct direction (arrow 1) and is guided along the circular track, jumping over narrow gaps (arrow 2). By contrast, a cell moving in the incorrect direction moves out of the circle but enters a neighboring circle in the correct direction (arrow 3). **(c)** Overlay of five consecutive fluorescence micrographs taken at 0.33 s intervals. The color gradient shows the counter-clockwise rotation of all 13 cells along the circular track (time sequence: yellow to orange to red). **(d)** A magnified view of the entrance to a circular track. The sharp end has a curvature radius of 50 nm and allows cells to move straight to the adjacent line. Scale bar, 1 μ m. **(e, f)** Aligned “crescent” and “tear drop” patterns. The

aligned asymmetric patterns function as one way gates that allow cells gliding along the pattern walls to move from the right to the left, but not the other way. (g) One-way gating of *M. mobile* cells between two closed areas using the aligned crescent pattern. (h) Accumulation of *M. mobile* cells against a density gradient using crescent-pattern one-way gates: 76% of the cells were concentrated in the left square after 20 min of movement. All scale bars are 5 μ m except panels a and d.

Figure 4

Transport of microbeads by *M. mobile* cells. (a-e) Scanning electron micrographs of *M. mobile* cells attached to 0.5 μ m microbeads. *M. mobile* cells attached one bead at the rear (b), front (c), or along the side (d), or two beads along both side of the cell body (e). (f-k) Overlays of sequential micrographs of cells carrying a 0.5 μ m micro-bead(s), taken at 1.0 s intervals. Covalently biotinylated *M. mobile* cells caught the streptavidin coated micro-bead(s) and carried it over the surface.

Unloaded (**f**) or cells carrying one bead at the rear (**g**), front (**h**), center (**i**), or along the side (**j**), or a cell carrying two beads (**k**) are shown. The gliding speeds of *M. mobile* cell were not affected by attaching the microbead(s). See supplementary Video 4.

Fig. 1

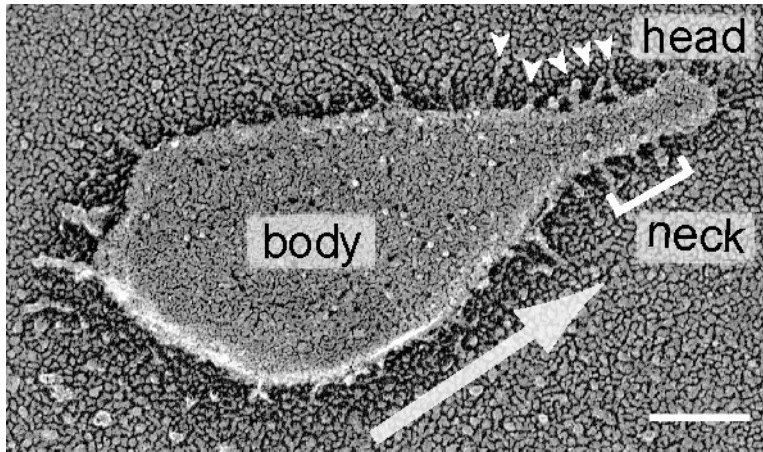


Fig. 2

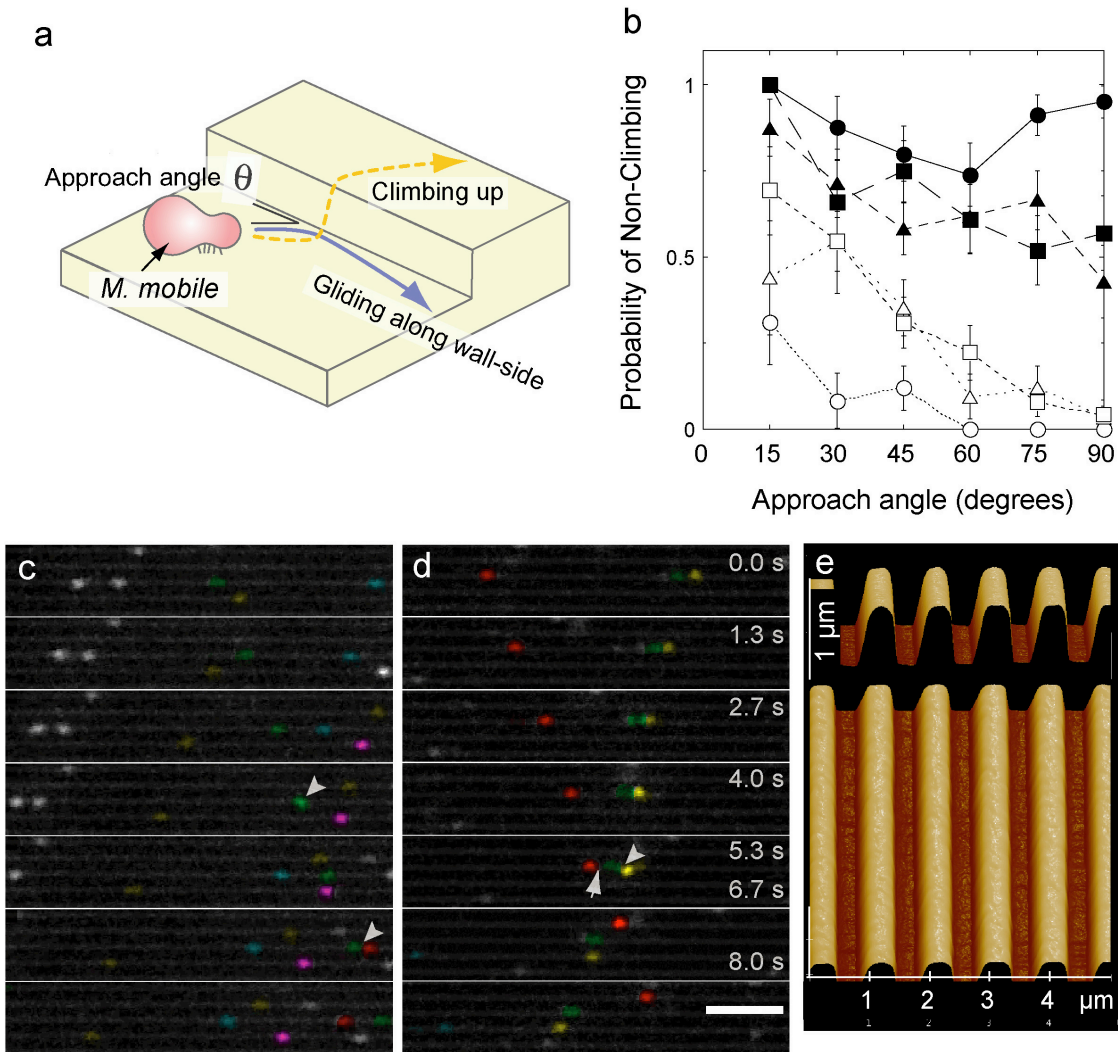


Fig. 3

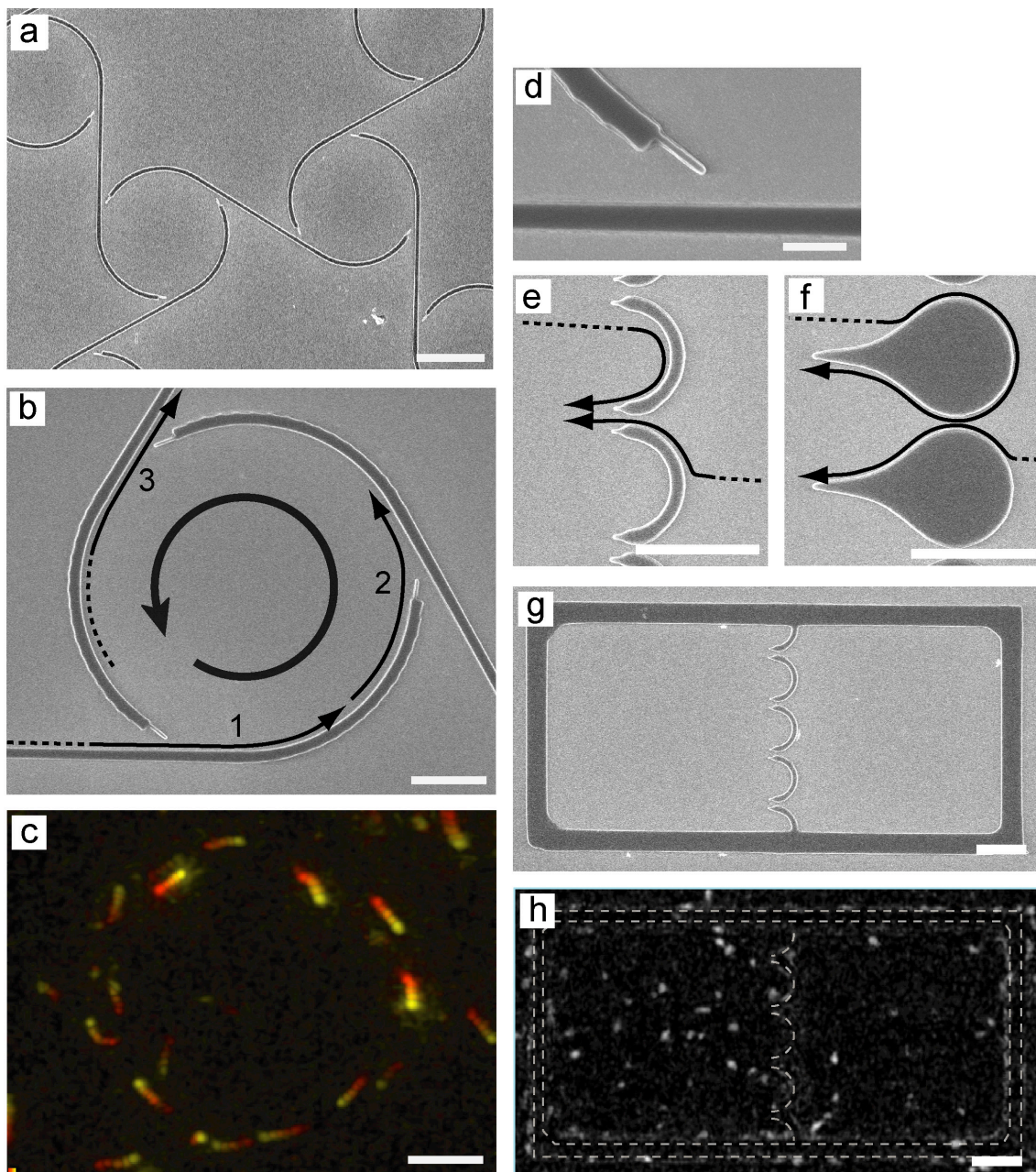
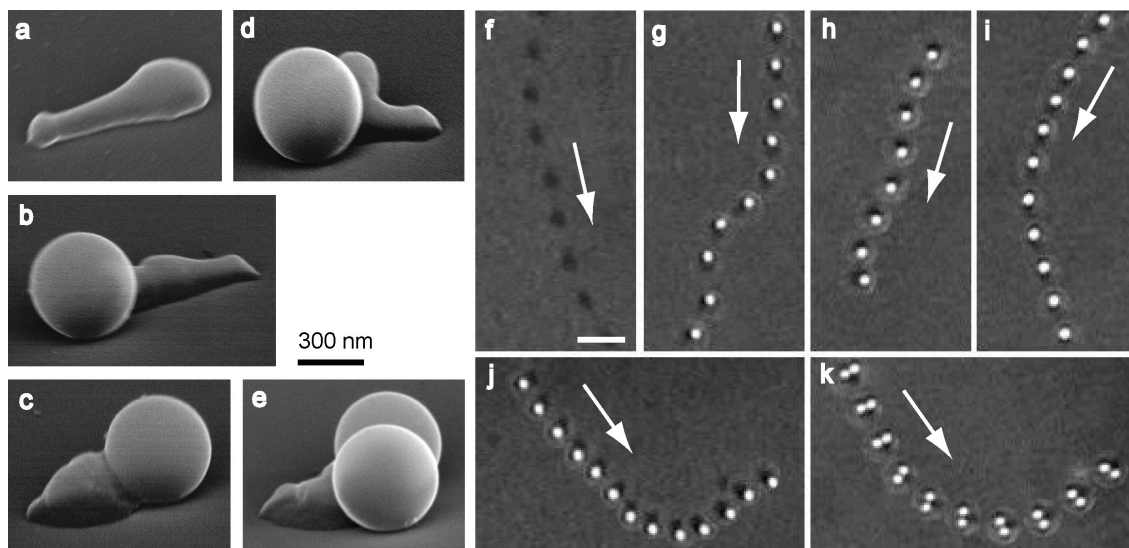


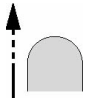
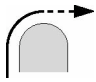

Fig. 4



TABLES

Table 1

Behavior of *M. mobile* cells moving along curved patterns with various curvature radii

Radius of curvature (μm)	Straight* ($< 30^\circ$) 	L-turn† ($30 \sim 120^\circ$) 	U-turn‡ ($> 120^\circ$) 
0.05	$62.4 \pm 10.1 \%$	$36.7 \pm 10.1 \%$	$0.9 \pm 2.1 \%$
0.25	$25.7 \pm 6.1 \%$	$71.3 \pm 8.8 \%$	$2.5 \pm 3.5 \%$
2.5	0 %	$19.7 \pm 4.2 \%$	$80.3 \pm 4.2 \%$
10.0	0 %	$3.6 \pm 7.2 \%$	$96.4 \pm 7.2 \%$

M. mobile cells were allowed to move along patterns that consisted of straight lines leading to outward 180-degree curvatures with various radii, and their behaviors were classified into three categories: * cells that moved straight or changed direction by less than 30 degrees and thus moved away from the pattern; † cells that glided along the curvature halfway and then

moved away from the pattern, resulting in a L-turn (between 30 and 120 degrees); and † cells that glided almost all the way along the curvature and then moved away from the pattern resulting in a near U-turn (between 120 and 180 degrees), or kept moving all the way along the curvature, resulting in a complete U-turn. That *M. mobile* cells responded differently to curves with radii $<0.25 \mu\text{m}$ and $>2.5 \mu\text{m}$ is likely related to their size.

Table 2**Comparisons between *M. mobile* and the kinesin/microtubule system as micro-transporters**

	<i>M. mobile</i>	kinesin / microtubule
Size	~1 μm	0.1~100 μm *
Energy Source	glucose [†]	ATP
Velocity	2~6 $\mu\text{m/s}$	0.5~1 $\mu\text{m/s}$ ‡
Force	~30 pN	6 pN x kinesin molecules §
Speed Control	temperature	temperature, chemical
Directional	Possible ¶	excellent
Control of Gliding		
Stability	robust	unstable **
Feature	self-repairing	very small
	self-reproductive	defined components
Potential	genetic engineering	protein engineering
	protein chemistry	protein chemistry

* This is the length of typical microtubule filaments polymerized *in vitro*.

The diameter of microtubules is 25 nm. [†] The energy source of the motor protein of *M. mobile* is still unknown, but *M. mobile* cells are able to synthesize the energy source by catabolizing glucose contained in the

medium. ‡ This is the speed of the conventional human brain or *Drosophila* kinesin that is most widely used in nano-biotechnological experiments. § The force generated by a single kinesin molecule is approximately 6 pN [32], but microtubules are usually powered by an ensemble of kinesin motors. || Native conventional kinesin is not known to have a regulatory system for its motor activity, except for cargo binding [33]. However, we recently used protein engineering methods to install a simple, Ca²⁺-sensitive chemical switch into conventional human kinesin (K. Konishi et al., manuscript in preparation). ¶ This paper. ** The lifetime is mainly limited by the stability of microtubules, rather than of kinesin. And the stability of microtubule is depends on the materials of the microtrack [34].